Semana Nacional de Engenharia Nuclear e da Energia e Ciências das Radiações - VII SENCIR
Belo Horizonte, 12 a 14 de novembro de 2024

Id.: CR-06

ARTIFICIAL NEURAL NETWORKS APPLIED IN THE CLASSIFICATION OF RADIONUCLIDES FROM GAMMA SPECTROSCOPY AND COMPUTATIONAL SIMULATION

Silva, Márcio M.A.[1], Azevedo, Ary M.[1], Nunes, Wallace V.[1], Morales, Rudnei K.[1], Cardoso, Domimingos O.[1]

[1] Instituto Militar de Engenharia, Rio de Janeiro, 22290-270, RJ, Brazil
marcio.magalhaes.br@gmail.com

Keywords: Neural Network (ANN), MCNP5, Gamma Spectroscopy

ABSTRACT

The present study seeks to develop a classifier of radioactive sources based on gamma spectroscopy and artificial intelligence, which makes use of Keras[1] and TensorFlow[2], both free and open-source technologies. Through these technologies, an artificial neural network (ANN) was developed, which makes use of supervised machine learning and the backpropagation algorithm. The neural network was trained with a dataset of spectra from simulations performed by the MCNP5 code. To achieve the objective of functioning as a classifier within the proposed scope, several versions of the neural network were evaluated, to study its performance, to determine important parameters such as a learning rate, and the optimizer used, among others, where RNA performance was evaluated by analyzing the network accuracy and loss curves. The generalization capacity was assessed by submitting spectra raised experimentally by an apparatus composed of a NaI (Tl) detector, a multichannel analyzer, and the Maestro software for the experimental data acquisition, which were used with the use of sealed radioactive sources of Co-60, Cs-137, and Eu-152. Six versions of the ANN were selected, capable of solving the proposed problem, with accuracy greater than 95%.

1. INTRODUCTION

It is notable in the literature the applications of Artificial Neural Networks (ANN) acting as classifiers in diverse fields, including the classification of radionuclides. ANNs are computational mathematical models inspired by the learning dynamics of the biological brain, which is based on a network of nerve cells (neurons) and the connections they form among themselves, called synapses. Likewise, ANNs are formed by interconnections between artificial neurons, called perceptrons. This model establishes numerical weights between these connections (synapses), allowing the network to learn by updating these weights, similarly to the biological learning process [3].

A radionuclide can be characterized by its gamma emission spectrum, which is formed by counting each gamma emission energy from a given radionuclide and ordering these counts by emitted energy. The spectrum can be represented by a graph where the x-axis represents the energy scale of gamma emissions (in keV) and the y-axis represents the count of each energy band obtained by the detection system [4]. To generate this spectrum, a detection system with a sensor capable of transforming the incident radiation energy into an electrical pulse proportional to that energy is required [5].

This methodology involves the use of ANNs and Supervised Machine Learning for the classification of radionuclides based on their gamma spectroscopy, utilizing simulation data from the MCNP5 code for training and testing the classifier. The classifier is then fed with spectrum data obtained from experimental apparatus not seen during training to evaluate the classification results.

One key application of this approach is the development of portable, personal-use systems that can be applied in various vehicles. These systems provide real-time radionuclide classification and monitoring, offering practical solutions for field operations, emergency response, or personal safety devices in radiation-prone environments [6]. Furthermore, such systems can help reduce unnecessary exposure to radiation for occupationally exposed individuals by providing timely and accurate detection of radioactive materials [7]. The following section will describe the steps taken to achieve these results.

2. METHODOLOGY

The methodology consisted of two phases, the first of which was aimed at setting up an experimental apparatus for surveying the spectra of nuclides Co-60, Cs-137, and Eu-152 at reproducing this apparatus in the MCNP5 computational simulation environment. The second phase of the study was dedicated to the study of the classification of radionuclides based on gamma spectroscopy, through the use of Artificial Neural Networks. The first phase entails the subsequent processes: (i) Installation of experimental apparatus and inspection of Co-60, Cs-137, and Eu-152 spectra with the use of a NaI(Tl) detector; (ii) Reproduce the experimental apparatus in a computational simulation environment of MCNP5 code; and (iii) Verification of simulated spectra the use of comparative evaluation of experimentally received spectra. The second phase primarily involves: (i) Setting up and training the initial ANN model utilizing the Keras framework; (ii) Examining the metrics linked with the implementation of neural networks that were configured and trained in the previous stage; (iii) Analyzing the outcomes; and (iv) Evaluating the ANN for the radioisotope spectra utilized in experimental surveying.

2.1. First Phase

The experimental equipment used in this phase consisted of: (i) a Sealed source of Co-60 with nominal radioactivity of 41 kBq, production statistics from 17 April 2007; (ii) A sealed source of Cs-137 with a nominal radioactivity of 37.4 kBq, with production statistics as of April 17, 2007; (iii) A sealed source of 152 Eu with a nominal radioactivity of 159.7 kBq, production statistics as of March 7, 2007; (iv) A set consisting of a scintillator detector, NaI(Tl), and a Canberra model 8023X3 photomultiplier tube valve with a Canberra model 2007 base; (v) Ortec preamplifier, model 113; (vi) Cambera amplifier, model 2022; (vii) MCB Ortec module, model 926; (viii) Ortec high voltage source, model 556; (ix) BIN Ortec, model 4001C; (x) Tektronix model TBS1064 oscilloscope; (xi) Amprobe Multimeter, Model HD110C; (xii) MCB Cable, Model DPMUSB; (xiii) Computer; and (xiv) ORTEC Maestro™ software, Version 7.01.
The apparatus used in the experiment with the NaI(Tl) detector consists of a rectangular wooden base 27 cm long, 23 cm wide, and 2.5 cm thick, and a central perforation 7.6 cm in diameter. There are four lead ring structures surrounding the sensitive volume of the detector, with outer and inner diameters of 15.2 cm and 8.26 cm, respectively. These structures encircle the area of incident radiation, except for the upper portion of the sensitive volume. The last lead ring is supported by a wooden stand consisting of a wooden disc with a diameter of 13.6 cm and carried by two identical rods with heights, widths, and thicknesses of 7, 3 cm, 9 cm, and 1.3 cm, respectively, made of wood. There is a perforation in the center of the wooden disk, with a diameter of 5.2 cm, and above it, there is a fountain holder composed of two acrylic sheets that overlap each other, with a thickness of 0.2 cm each. The upper blade contains a central perforation of the exact diameter (2.6 cm) to accommodate the sealed cylindrical sources used in the experiment. The geometry and

chemical composition of the materials used in the apparatus are illustrated in Figure 1, where the colors represent the materials used. Details of detectors less than 2 mm thick have been removed from the front view for simplicity. It is represented by material number 4 and is illustrated in the figure concerning composition as materials 4. a, 4. b, and 4. c.

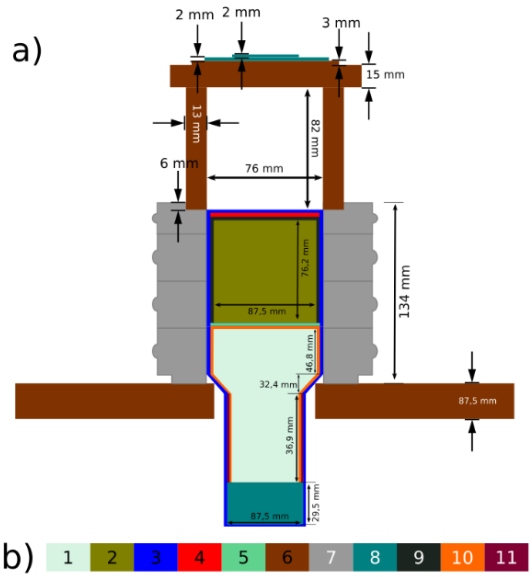

Mat.	Chemical Element	wt(%)	Density (g/ cm3)
1	Vacuum	-	-
2	Na	15,34	3,66
	I	84,66	
3	Al (100)	100	2,69
4.a	Al (100)	100	2,69
4.b	H	8	1,23
	O	52	
	Cl	40	
4.c	H	14,37	0,93
	C	85,63	
5	H	8,1	1,0185
	C	32,1	
	O	22,3	
	Si	37,5	
6	H	5,96	0,64
	C	49,7	
	N	0,5	
	O	2,74	
	Mg	0,2	
	S	0,5	
	K	0,2	
	Ca	0,2	
7	Pb	100	11,35
8	H	8,05	1,19
	C	59,99	
	O	31,96	
9	O	39,7	0,55
	Mg	60,3	
10	O	15,64	6,22
	Si	8,1	
	Tl	0,8	
	As	0,26	
	Pb	75,19	
11	C	0,0017	1,1805
	Fe	0,99	
	Mn	0,0075	
	P	0,00035	
	S	0,00045	

Figure 1. a) Schematic front view of the apparatus geometry; b) Chemical composition of the materials used, including their proportion in mass and density

The detector was powered by a high voltage source with a voltage of 750 V. This voltage was roughly set to 500 V by the 6-position switch control, 200 V by the 5-position switch control, and 74 V by the 10-turn precision potentiometer. The tweaks were made by measuring with a multimeter before switching on the detector. The NaI (Tl) detector diode output was connected to the preamplifier input with capacitance set to 0 μF. Following that, the signal output of the preamp is connected to the input of the amplifier. Then, the output of the unipolar amplifier is connected to the input of the MCB module and is equipped with a T-piece. This allowed the signal from the amplifier to be captured by the oscilloscope, to enable fine-tuning of the shaping parameters to 0.5 μs, coarse gain to a value of 100, and fine gain to a value of 0.33. The tuning was done by visual analysis of the pulses obtained after assembling the device using a Co-60 source placed inside the device and attempting to maximize the pulse height without saturating it. Tweaks were made in the P / Z controls (pole-zero) to eliminate the small undershoots that formed during the adjustment. Adjusted the shaping control by checking the generated pulse width for better symmetry. The MCB module was set to a low window of 0.5V (LLD setting) and the zero control was set to 0V. The module was then connected to a computer via a DPM USB cable, and spectroscopic data was received by the Maestro Software.

The simulation phase with MCNP5 code consisted of reproducing the shape of the NaI (Tl) detector described in this section. After the geometry was simulated, three MCNP5 input files were

developed. Since these files differ only in the composition of the radiation source, the simulation reproduces the spectra of the three radionuclides used. Geometric element, cell, and source construction was performed according to the definition in the MCNP documentation [8], [9].
The source was configured as a fixed plane, and the composition of the MCNP5 input file was based on theoretical energy mapped from the Laraweb database [10]. The reproduction distance between the source and the detector was 110 mm. The F8 tally of MCNP5 is used to generate the output file using the simulated spectrum, using the GEB function with parameters a, b, and c set to −9.3408× 10−3, 7.5107× 10−2 and 0.5843 respectively, with a reliability criterion of relative error less than 0.1. Some modeling points, such as modeling the parameters, materials, and detectors used in the GEB function, are based on MEDEIROS work [11]. The simulation was run on a computer with an Intel® Core™ i7 8700 3.2 GHz processor (6 physical cores and 12 logical cores), 8 GB RAM, and running the 64-bit version of the Windows 10 Home operating system.
It should be noted that all the studies were conducted using the liquid spectrum, which was obtained by subtracting the background radiation from the experimental spectrum, to disregard the background radiation in computer simulations. This simplification was intended to reduce the number of variables in the study and to facilitate the generation of a simulated spectrum.

2.2. Second Phase

The second phase started from an already validated ANN architecture (NUNES [12]), which originated five other versions of ANN, resulting from successive alterations of the architectural hyperparameters, to improve the classification performance of these networks. The loss and accuracy curves are key to the test dataset to guide the comparison of classifier performance between ANN versions. From this point of view, the goal is to make the final accuracy of the ANN as high as possible and to minimize the loss (or error). It is important to highlight that, before being used as training, tests, and production data of the ANN, both the simulated spectra and those obtained experimentally, which originally have 8192 channels, were sampled for 128 channels, aiming at compatibility with the number of neurons in the ANN. input layer of the networks, to provide the reduction of the computational cost during the processing of the experiments.
The initial configuration of the ANN assumes a three-layer (one hidden layer) network architecture, the first layer with 128 neurons using the hyperbolic activation function, the second layer with 64 neurons using the complementary Gaussian activation function, and the third layer using the logistic activation function with 3 neurons. In this model, a learning rate of 0.1 was used and an SGD optimizer with a momentum equal to 0.44, using 3600 training epochs. The ANN model was implemented in Python [13], using Keras [1] and Tensorflow [2].
The second version of ANN consists of a first variation in the parameterization of the base model that was performed by changing the activation function of the last layer by the softmax function, because it transforms the output vector into a probabilistic representation, making the results more intuitive.
From the third version, there was an extended ANN's knowledge base. This process was performed using a computer simulation model to obtain simulated spectra of other target nuclides listed in the inventory shown in Table 1, including a total of 24 radionuclides. The nuclide selection is based on a study of CURZIO [14], which obtained a radionuclide inventory resulting from a simulation of an accident involving a small DWR reactor using the SCALE code, and PEREIRA [15], which, in their study, evaluated the radioactive effects of a Radiological Dispersion Device (RDD), also known as a dirty bomb, through computer simulation.

In this phase, only the number of neurons in the output layer is changed to 24 because the number of radionuclides under investigation has increased. From that point onwards, subsequent versions of the ANN underwent experimental definition of hyperparameters until the classification of the experimental spectra for the radionuclides Co-60, CS-137, and Eu-152 was achieved.

Source	Half-life	Source	Half-life	Source	Half-life
Ba-140	12.753 d	Cs-137	30.05 y	U-238	$4.468x10^9$ y
I-131	8.0233 d	Co-60	5.2711 y	U-235	$704x10^6$ y
I-135	6.57 h	Am-241	432.6 y	K-40	$1.2504x10^9$ y
Kr-85m	4.480 h	Ra-226	$1.600x10^3$ a	Th-232	$14.02x10^9$ y
Te-132	3.230 d	Ir-192	73.827 d	Eu-152	13.522 y
Xe-133	5.2474 d	Pu-238	87.74 y	Ba-133	10.539 y
Xe-133m	2.198 d	Po-210	138.3763 d	Co-57	271.81 d
Xe-135	9.14 h	Cf-252	2.6470 y	Mn-54	312.19 d

Table 1. Radioactive sources used in the simulations [10]

During this phase, experiments were performed to determine the learning rates and learning momentum [3]. After adjusting these parameters, an experiment based on the comparative KINGMA study [16] was performed to define the optimizer used in the network. The parameter that determines the choice is an analysis of the loss function related to the number of training epochs, choosing the optimizer that reduces the loss function most quickly concerning the learning period.
Once the learning rate, momentum (if applicable), and optimizer to be used are determined, each parameterization is subject to a graphical analysis to examine the relationship between the test and training datasets and their associated loss functions. This analysis is crucial as it validates the possibility of overfitting [17]. In cases where overfitting signals were identified, the training method with early stopping in the network was used. In that phase, the experimental nuclides used in the study were best classified, and networks with at least 95% accuracy were considered viable. The study results will be shown in the next section.

3. RESULTS AND ANALYSIS

Similarly to the methodology section, the results followed the same division into two phases used in the methodology, to facilitate the understanding of the workflow of activities.

3.1. First Phase Results

The first phase of this study presents the results obtained from energy calibration of the experimental apparatus, passing through the experimental survey of the spectra of Co-60, Cs-137, and Eu-152, as well as the simulation of the experimental apparatus with the use of the MCNP5 code.
Energy calibration was performed by surveying the spectra of the three radionuclides used, using the Maestro software, which supports up to 96 calibration energies, and the Laraweb radionuclide database [10], considering only energies with intensities above 10%. The calibration process began with Eu-152, which has the highest energy among the nuclides. Then, Cs- 137 and Co-60 were used in the process. It is worth noting that, due to the energy resolution of the detection system used, only six energies with intensities above 10% could be distinguished for Eu-152. The three spectra were surveyed without variation of the experimental and electronic devices, with a live time

of 3600 seconds, with an average dead time of less than 10%. The calibration curve was adjusted by the equation $Y = 0.208X_i - 9.553$, where X_i is the ith channel of the spectrum.
Regarding MCNP5 code simulation, it was verified that the comparison between the experimental and simulated spectra was satisfactory, especially in the approximation of the characteristic energy peaks of each spectrum. This analysis was performed visually, through the superposition of experimental and simulated spectra, for each radionuclide.

3.2. Second Phase Results

The first ANN version was carried out using the spectra obtained through the simulation of the experimental apparatus by the MCNP5 code, as training and test data, for the spectra of Co-60, Cs-137, and Eu-152. As production data, to evaluate the quality of the generalization capacity of the model were used the experimental spectra were surveyed with the NaI(Tl) apparatus, described in the methodology section.
This initial validation aimed to verify if the visual similarity between the experimental and simulated spectra was reflected in the classification capacity of the network, as represented by the first version of the ANN file. The values of the loss and accuracy can be viewed in Table 2, as well as its separation in classes. The values of accuracy and loss in the last training epoch obtained were 100% and 2.0605×10^{-4}, respectively.
The second version of ANN, in which the activation function of the output layer was changed to a softmax function, generated the final values of accuracy of 100% and loss of 1.5760×10^{-4}, as can be viewed in Table 2. Also can be viewed in this table the results of the separation into classes of the model, which show an improvement in changing the activation function of the last layer in reducing the final value of the loss function.

ANN Vers.	Co-60(%)	Cs-137(%)	Eu-152(%)	Loss	Accuracy(%)
First	08.19	23.79	12.45	2.0605 × 10−4	100.00
Second	99.93	99.83	98.25	1.5760 × 10−4	100.00
Third	78.14	40.53	86.65	0.6872	85.41
Fourth	69.92	89.46	3.52	0.4029	91.66
Fifth	99.84	97.45	96.19	0.4763	95.83
Sixth	100.00	98.97	99.14	2.7680 × 10−3	95.83
Seventh	99.87	99.99	99.88	0.188466	95.83

Table 2. Classification, loss, and accuracy results by all ANN versions

Concerning the third version of the ANN, it was observed that the probability related to submission of the Cs-137 experimental spectrum was only 40.53%, which required the network to refine its parameterization. It was verified that the loss function had high values in relation to the second ANN version (approximately 0.6872 for the third ANN version against the final loss value of 1.5760× 10−4 obtained in the training of the second ANN version), due to the increase in the number of classes in the network's training dataset.
The fourth ANN version was obtained with an experimental variation in momentum and learning rate parameters. The learning rate reflects the number of steps that the loss function takes to reach a local minimum. Thus, the order of magnitude has been reduced from 10−1 to 10−2, to observe the behavior of this ANN version. However, the change in the learning rate must take into account its

relationship with the momentum, as it contributes to the rate of fall of the loss function curve. To determine a momentum value that best fits the learning rate of 10−2, a comparison between training performed with the fourth ANN version was performed, observing the drop speed of the loss curve, with the momentum value varying between 0.5 and 1.0. The value that had the best performance according to the established criterion was 0,95. The classification results and the values of metrics of this ANN version are shown in Table 2, where it can be seen that the classification is still erratic in relation to Eu-152, and the loss function has fallen but is still in high value considering the second ANN version, remaining at approximately 0.4029. The accuracy at the end of the training was 91.66.

Refining the network parameterization, an empirical analysis was also carried out between the performance of the optimizers available in Keras, in the same way as the study carried out by [16], based on the architecture of the fourth ANN version. Thus, a comparison was made between the loss curves between network training, with the number of epochs set at 200, with Adam being the optimizer that had the best performance, as illustrated in figure 2 (In addition to Adam, the optimizers Adadelta, SGD, SGD Nesterov, RMSprop, and Adagrad were tested).

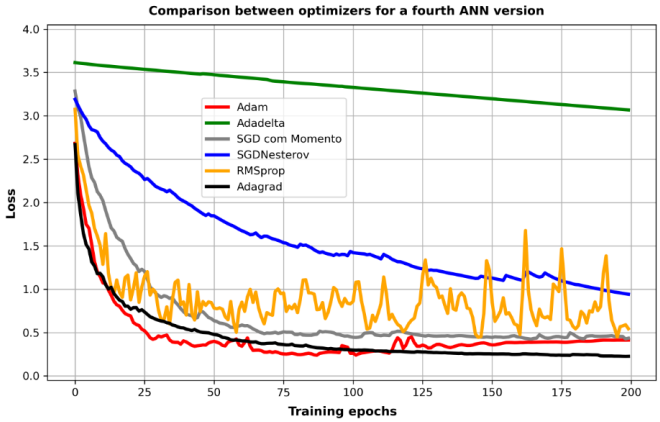

Figure 2. Definition of optimizer with fourth ANN version

Therefore, the optimizer used by Keras was changed from SGD (Stochastic Gradient Descent) to Adam. This time there was a reduction in the loss function, to the approximate value of 0.4763. The classification became assertive in relation to the 3 tested nuclides. The fifth ANN version file refers to the network version after the optimizer change, while the classification results and the metrics values are displayed in Table 2. The accuracy after the end of training was 95.83%. The result obtained with the fifth ANN version matched the objective of the study, proving to be a viable network to be used as a classifier within the premises established for the study. However, it was still possible to experimentally evaluate the impact of altering some network parameters described below. Analyzing the curves of the training and testing loss functions of the fifth.

ANN version, as shown in Figure 3, a behavior that would represent their loss of the ability to generalize was detected [3], being a conditional situation to the use of early stopping. The use of early stopping shows that the fifth ANN version can be assertive in relation to the classification of the nuclides obtained experimentally, with the training carried out with only 313 epochs, reaching

a loss of 0.340864, less than the loss of 0.476314 of the training carried out with 3600 epochs, obtaining the same accuracy of 95.83%. Therefore, the aforementioned model can be considered as being viable for the classifier.

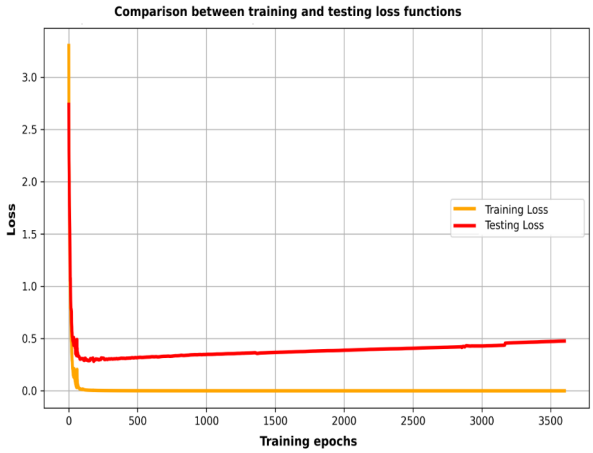

Figure 3. Analysis of the curves of the training and testing loss functions of the fifth ANN version

The next parameter evaluated, according to the sequence established in subsection 2.2, was the training batch size (batch size). The batch size was increased from 32 to 128, with this change being the sixth ANN version. The results of the separation into classes of the production data for the sixth ANN version are shown in Table 2, as well as the metrics values. The sixth version of the ANN also matched the criteria established for the study, being considered a viable model for the classifier. The analysis of the training and test loss function curves of the sixth version of the ANN also showed a characteristic behavior of the overfitting indicator. Therefore, a study was carried out, similar to the one done for the fifth version of the ANN, including the early stopping option. It was observed that the sixth ANN version model, trained with 101 epochs, already becomes a viable model, reaching 95.83% accuracy, having a loss value at the end of training of 0.002768, much lower than the loss of 0.316896 of training with 3600 epochs, keeping the same accuracy of 95.83%. In addition, the classification was assertive in relation to the nuclides submitted to the classification, with percentages above 93.58%.

Following the sequence established in subsection 2.2, the seventh ANN version network underwent the inclusion of a second hidden layer, using the same activation function of the first hidden layer (complementary to the Gaussian). After performing the training, there was no improvement in the classification probability percentages of the experimental spectra of radionuclides Co-60, Cs-137, and Eu-152, which are tabulated in Table 2. The values of final loss and accuracy observed were 0.188466 and 95.83%, respectively, and the curves can be viewed in Figure 4. The seventh version of the ANN also matched the criteria established for the study, being considered a viable model for the classifier. Although the analysis of the seventh ANN version training and testing loss function curves, as performed in the fifth and sixth versions, does not show a behavior indicative of over-fitting. However, early stopping was applied to check the experimental result resulting from the

test, following the methodology established for this work. Was observed that the seventh ANN version model trained with 273 epochs presents itself as a viable model, reaching 95.83% of accuracy, with a loss value at the end of training of 0.300991, higher than the value of 0.188466 obtained by training the network with 3600 epochs, although it maintains the same accuracy of 95.83%. Nevertheless, the probability presented by the submission to the classification of Eu-152 dropped from 99.88% to 94.40%. Thereby, six ANN models are viable for the classifier, represented by the fifth, sixth, and seventh ANN versions, and its derivative models obtained by an early stopping training.

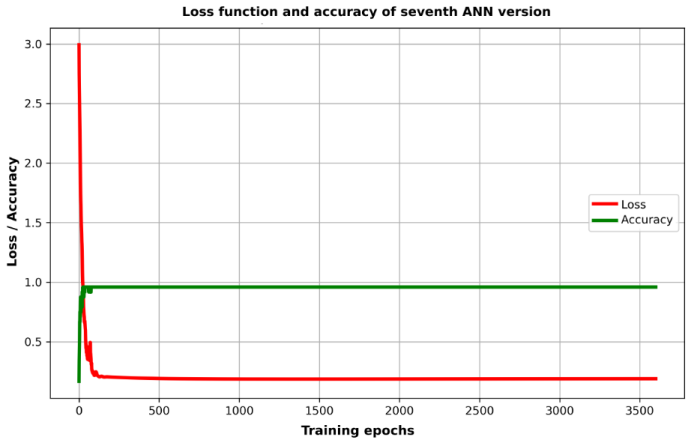

Figure 4. Loss and accuracy curves of the seventh ANN version

4. CONCLUSIONS

The work showed how feasible the use of artificial intelligence, more specifically of supervised machine learning, is through the application of Artificial Neural Networks (ANN) for the development of automated classifiers of radioactive sources. The developed classifier was able to distinguish the radionuclides Co-60, Cs-137, and Eu-152, based on gamma spectroscopy, having its training carried out based on an inventory of simulated gamma spectra of 24 radionuclides. The geometry of the experimental apparatus illustrated in section 2.1 was reproduced within the MCNP5 code so that the data extracted from the simulation could be used in the training and testing sets of the studied ANN versions. The evolution of the classifier was carried out through changes in the main parameters of ANN, based on the observation and analysis of the behavior of the loss and accuracy functions, used as metrics to assess the quality of the classifier. The study allowed the understanding of the operation of equipment and systems available on the international market, with similar functionality, even if the implementation of their software uses classification algorithms different from the ANNs. This shows that, in addition to understanding how spectra classifiers work, a viable solution was found for the application in question. It should also be noted that the uncertainties regarding the classification of the experimental spectra of the sources, shown by the classifier of this study, even in a controlled environment, also occur in commercial products with the same purpose, since the classification of spectra requires the analysis of several parameters such as geometry, influence of background radiation, presence of other radioactive sources in the sample, among other factors. Among many parameters present in the ANN implementation carried out using the Keras library and TensorFlow, it was observed that special attention is needed regarding the learning rate, the

optimizer used, the training batch size, and the number of hidden layers of the network. Among the models studied, it was found that 6 of them are viable models for use as classifiers within the scope defined for this study, with accuracy above 95%, and with good generalization ability in relation to the 3 experimental spectra used in the study. It is expected that this generalization capability will be valid for other spectra, among those present in the simulated spectra used as training data for ANN versions. Thus, it is expected that the present study takes a step towards increasing autonomy in the design of this type of detector, and in its applications for Radiological and Nuclear Defense (DRN).

ACKNOWLEDGEMENTS

We would like to express our deep gratitude to the Instituto Militar de Engenharia (IME), especially the departments of Nuclear Engineering and Materials Engineering and Sciences, for their significant contribution to the advancement of science and technology in Brazil. The commitment and excellence of these departments are fundamental for the development of innovative research and the training of highly advanced professionals.
Furthermore, I would like to thank the funding institutions, such as the Coordination for the Improvement of Higher Education Personnel (CAPES) and the National Institute of Educational Studies and Research Anísio Teixeira (INEP), for the financial and institutional support that made it possible to carry out our research projects and high-level human resources training.

References

[1] F. Chollet, "Others keras [internet]", *GitHub*, 2015.
[2] M. Abadi, P. Barham, J. Chen, *et al.*, "{Tensorflow}: A system for {large-scale} machine learning", in *12th USENIX symposium on operating systems design and implementation (OSDI 16)*, 2016, pp. 265–283.
[3] S. Haykin, *Neural networks and learning machines, 3/E*. Pearson Education India, 2009.
[4] N. Tsoulfanidis and S. Landsberger, *Measurement and detection of radiation*. CRC press, 2021.
[5] G. F. Knoll, *Radiation detection and measurement*. John Wiley & Sons, 2010.
[6] T. d. M. S. Silva, A. C. L. Lobato, A. K. F. Mendonça, *et al.*, "Application of area monitors and scintillating detectors in the development of cbrn defense reconnaissance vehicles", *Brazilian Journal of Radiation Sciences*, vol. 9, no. 3, 2021. doi: https://doi.org/10.15392/bjrs.v9i3.1698.
[7] A. de Azevedo, J. Gonçalves, A. Salazar, *et al.*, "Radiometric survey with remotely piloted land vehicle in chemical, biological, radiological and nuclear defense operations", *Brazilian Journal of Radiation Sciences*, vol. 11, no. 1A (Suppl.) Pp. 01–13, 2023. doi: https://doi.org/10.15392/2319-0612.2023.2184.
[8] J. F. Briesmeister *et al.*, "Mcnptm-a general monte carlo n-particle transport code", *Version 4C, LA-13709-M, Los Alamos National Laboratory*, vol. 2, 2000.
[9] J. Shultis and R. Faw, "An mcnp primer department of mechanical and nuclear engineering", *Kansas State University*, 2010.
[10] N. Lara, *Library for gamma and alpha emissions*, 2023.
[11] M. P. Medeiros, *Gamma absorption coefficients calculation by NaI(Tl) detector and computer modeling in MCNPX code*. Associação Brasileira De Energia Nuclear, 2015.

[12] W. Nunes, A. da Silva, V. Crispim, and R. Schirru, "Explosives detection using prompt-gamma neutron activation and neural networks", *Applied Radiation and Isotopes*, vol. 56, no. 6, pp. 937–943, 2002, issn: 0969-8043. doi: https://doi.org/10.1016/S0969-8043(02)00059-3. [Online]. Available: https://www.sciencedirect.com/science/article/pii/S0969804302000593.

[13] G. Van Rossum, F. L. Drake, *et al.*, *Python reference manual*. Centrum voor Wiskunde en Informatica Amsterdam, 1995, vol. 111.

[14] R. C. Curzio, A. T. Neto, B. da Silva Moura, *et al.*, "Modelagem computacional da dispersão atmosférica aplicada a um reator modular de pequeno porte", *Brazilian Journal of Radiation Sciences*, vol. 9, no. 1, 2021. doi: dx.doi.org/10.15392/bjrs.v9i1.1244.

[15] J. F. Pereira, "Explosão de bomba suja em local de grande evento público: Uma metodologia para ações de emergência radiológica", *Comissão Nacional de Energia Nuclear Instituto de Radioproteção e Dosimetria*, 2018.

[16] D. P. Kingma and J. Ba, "Adam: A method for stochastic optimization", *arXiv preprint arXiv:1412.6980*, 2014.

[17] F. Chollet, *Deep learning with Python*. Simon and Schuster, 2021, isbn: 9781617294433.